Dynamics of moments of FitzHugh-Nagumo neuronal models and stochastic bifurcations

Seiji Tanabe
Department of Systems and Human Science, School of Engineering Science, Osaka University, Toyonaka, 560-8531 Osaka, Japan

K. Pakdaman
Inserm U444, Faculté de Médecine Saint-Antoine 27, rue Chaligny 75571 Paris Cedex 12, France

(Received 1 September 2000; published 27 February 2001)

For the study of the behavior of noisy neuronal models, Rodriguez and Tuckwell have introduced an elegant and systematic method which consists of replacing the system of stochastic differential equations with a system of deterministic equations representing the dynamics of the means, variances, and covariance of the state variables [R. Rodriguez and H.C. Tuckwell, Phys. Rev. E **54,** 5585 (1996)]. In this work, we first report a modification of their method in the case of the FitzHugh-Nagumo model which enhances the accuracy of the approximation without including higher order moments. This method is then combined with a self-consistency argument in order to better characterize the behavior of the underlying stochastic processes through the computation of approximate auto- and cross-correlation functions of the state variables. Finally, we argue that the moments' equations can also reveal the existence of stochastic bifurcations, i.e., qualitative changes in the dynamics of stochastic systems.

DOI: 10.1103/PhysRevE.63.031911 PACS number(s): 87.10.+e, 07.05.Mh

I. INTRODUCTION

Noise can significantly alter the response of neurons and it has been postulated that this effect may play a functional role in signal processing in nervous systems [1]. This has in turn motivated theoretical investigations aiming to determine the mechanisms underlying the influence of noise, using a wide variety of models and approaches [2,3], such as, for instance, first passage time analysis of integrate-and-fire models [4,5] and other reduced stochastic models [6], and mean firing rate approximations of FitzHugh-Nagumo (FHN) and Hodgkin-Huxley (HH) models [7,8].

In a previous study [9], we reported a different class of noise induced phenomena by examining the influence of noise directly on the membrane potential of the HH model, rather than on its discharge rate. More precisely, we observed that, at low noise levels, the stationary membrane potential distribution takes on a Gaussian form clustered around the resting state, while at high noise intensities, it takes on a bimodal form stretching out well beyond the firing threshold, with the transition between the two regimes taking place in a relatively narrow range of noise. Furthermore, we argued that such a noise induced change in the membrane potential distribution could be of functional significance because it was responsible for the noise enhanced discharge timing precision reported by Pei *et al.* [7].

However, despite evidence of its significance, to our knowledge the main analysis of such noise induced transitions remains based on numerical investigation. The purpose of this paper is to develop a semianalytical method to capture such noise induced changes and illustrate it by showing that the FHN model also undergoes a noise induced transition similar to the HH model.

The main guiding point in our analysis is that the noise induced transition in [9] is strongly reminiscent of phenomenological stochastic bifurcations [10], that is when, in a stochastic system, the change in a parameter value leads to a qualitative change in the stationary solution of the corresponding Fokker-Planck equation. However, the analysis of such bifurcations remains arduous as there are no general algebraic characterizations of such changes as there exist, for instance, for describing local bifurcations of deterministic systems. Nonetheless, this suggests that it may be possible to capture phenomenological stochastic bifurcations as deterministic bifurcations in an appropriately defined deterministic approximation. The purpose of the present work is to define such an approximation and apply it to the study of the stochastic bifurcation of the FHN model as the noise intensity is increased.

Our starting point is Rodriguez and Tuckwell's (RT's) efficient and systematic method to compute the dynamics of the moments of the model variables [11–13]. More precisely, their approach was to assume that when the fluctuation is small, the distribution of the state variables of a system takes on a Gaussian shape. Under this assumption, statistical estimates sampled from simulations of a large network of coupled stochastic differential equations are replaced with a system of purely deterministic differential equations for the first and second order moments. They have formulated the moments' equations successively for a general system [11], the FHN model [12], and the HH model [13]. In all models, their approximation proved to be in excellent agreement with transient behavior of simulations of the stochastic system at low noise amplitude. However, as they have pointed out, their approximation may break down after some time duration. For this reason, their method is not optimally suited for analyzing the asymptotic behavior of noisy neuron models. We therefore start by modifying their method to adapt it to the analysis of stationary distribution of state variables in excitable noisy neuron models. Then, we show that deterministic bifurcations in these revised moments equations can be used to characterize the phenomeno-

logical stochastic bifurcation in the noisy FHN.

This paper is organized as follows. First, we compare our modified moments equation of the FHN model with RT's original equations in Sec. II. Second, in Sec. III, we examine the self-consistency of moments equations, and using it, we compute auto- and cross correlations of the model variables. Third, we investigate the correspondence between the deterministic bifurcations of moments equations and the phenomenological stochastic bifurcation of the FHN in Sec. IV. Finally, we discuss the results in Sec. V. Furthermore, Appendix A is devoted to technical aspects pertaining to the moments equations.

II. MOMENTS OF THE FITZHUGH-NAGUMO MODEL

The standard FHN model receiving white Gaussian noise is described by the following stochastic differential equation,

$$\frac{dx}{dt}=A(x,y)+I+\xi(t),$$

$$\frac{dy}{dt}=B(x,y), \tag{1}$$

where functions $A(x,y)=ax^3+bx^2+cx+hy$ and $B(x,y)=ex+fy+g$ and the noise term $\xi(t)$ satisfies both $E[\xi(t)]=0$ and $E[\xi(t)\xi(s)]=\sigma^2\delta(t-s)$.

As a starting point, we remind Rodriguez and Tuckwell's (RT) method as applied to the noisy FHN model [14]. These authors first assume that the distributions of the variables take on approximately Gaussian forms so that they can be entirely characterized by their first and second order moments (i.e., the means, the variances, and the covariances). Then using a second order Taylor expansion of the expressions of the moments of x and y, and taking advantage of the fact that odd ordered moments are zero, they derive the equations for the moments as

$$\frac{dm_1}{dt}=F_1(m_1,m_2,S_1)=A(m_1,m_2)+\frac{1}{2}A_{xx}(m_1,m_2)S_1+I,$$

$$\frac{dm_2}{dt}=F_2(m_1,m_2)=B(m_1,m_2),$$

$$\frac{dS_1}{dt}=F_3(m_1,S_1,C_{12})=2[A_x(m_1,m_2)S_1+A_y(m_1,m_2)C_{12}]+\sigma^2,$$

$$\frac{dS_2}{dt}=F_4(m_2,S_2,C_{12})=2[B_x(m_1,m_2)C_{12}+B_y(m_1,m_2)S_2],$$

$$\frac{dC_{12}}{dt}=F_5(m_1,S_1,S_2,C_{12})=B_x(m_1,m_2)S_1+A_y(m_1,m_2)S_2+[A_x(m_1,m_2)+B_y(m_1,m_2)]C_{12}, \tag{2}$$

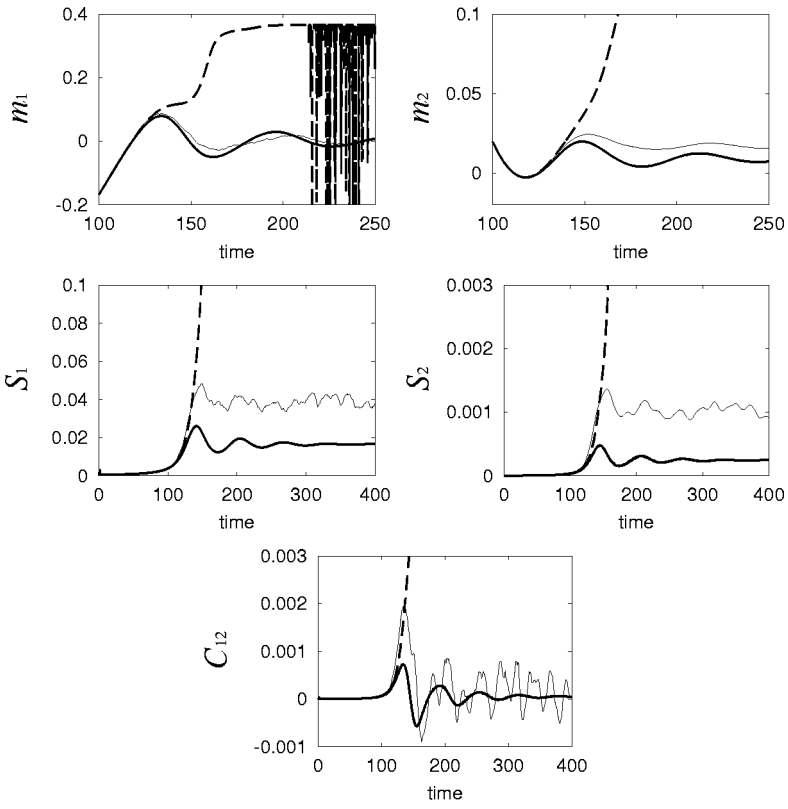

FIG. 1. Dynamics of moments derived under the RT and G method in an excitable FHN model. Time evolution of m_1 is shown in the top left panel. Each curve is the solution of the G method (thick solid lines), RT method (thick broken lines), and an estimate from simulations of 1000 units (thin solid lines). m_2 (top right panel), S_1 (middle left panel), S_2 (middle right panel), and $C_{1,2}$ (bottom panel) are plotted in respective panels. All abscissas are time in milliseconds and ordinates are in arbitrary units. Noise intensity $\sigma=0.05$ and constant current $I=0$. Model parameters were chosen to be identical with [12], that is, $a=-0.5$, $b=0.55$, $c=-0.05$, $e=0.015$, $f=-0.003$, $g=0$, and $h=-1$. Initial conditions were chosen $m_1(0)=m_2(0)=1$, and $S_1(0)=S_2(0)=C_{12}(0)=0$. The computations were carried out using the fourth order Runge-Kutta method with a time step of 0.1 for the approximations and the standard Euler method with a time step of 0.01 for the simulations. Similar results were obtained with smaller time steps.

where means $m_1=E[x]$ and $m_2=E[y]$ are the first order moments, and variances $S_1=E[(x-m_1)^2]$ and $S_2=E[(y-m_2)^2]$ and covariance $C_{12}=E[(x-m_1)(y-m_2)]$ are the second order moments. The functions A_x, A_y, A_{xx}, and so on, are the first and second partial derivatives with respect to x and y.

In our analysis, we follow RT's assumption that the distributions are approximately Gaussian, however, we evaluate the moments' equations in a different method. Rather than using the Taylor expansion, we take advantage of the fact that the functions A and B are polynomials, so that, under the Gaussian assumption, one can obtain the exact expressions of their moments in terms of the first and second order moments of the variables (Appendix A). We refer to this method as the G method to distinguish it from the RT method.

With the G method, we obtain a system of equations for the dynamics of the moments of the FHN in which the third and fifth equations differ from those in Eq. (2) as

$$\frac{dS_1}{dt}=F_3+6aS_1^2, \tag{3}$$

$$\frac{dC_{12}}{dt}=F_5+3aS_1C_{12}. \tag{4}$$

Given that, in the FHN model $a<0$, and that $S_1>0$ (it is a variance), the terms added to these equations oppose variations of S_1 and C_{12} because their partial derivatives with respect to S_1 [for the extra term in Eq. (3)] and to C_{12} [for the term in Eq. (4)] are negative. The addition of these dissipative terms has thus a stabilizing effect on the dynamics of S_1 and C_{12} and consequently on the whole system.

Figure 1 illustrates this point. The panels in this figure represent the temporal evolutions of the moments computed with either method (thick dashed lines for RT and thick solid lines for G), together with estimates obtained from 1000 simulations (thin solid lines). The three sets of lines remain close to one another during roughly the first 100 ms. This is in agreement with the statement that the RT provides an excellent approximation of the transient evolution of the moments. It also shows that the G behaves in a similar way. Nonetheless, the asymptotic dynamics of the two methods differ considerably. While the moments from the G method stabilize at steady states, either in good agreement with estimates from simulations (top two panels and bottom panel) or with some degree of underestimation (middle two panels), those from the RT method blow, or display growing oscillations.

The above example illustrates that the modification brought to the RT method renders it suitable for our purpose, that is, the analysis of the noise induced changes in the stationary distributions of the variables. In this respect, the fact that the G method underestimates quantitatively the second order moments is not of importance, because our interest is not in estimating the discharge rate of the model as in [12], but instead to characterize qualitative rather than quantitative changes in the steady state regime.

III. SELF-CONSISTENCY AND THE CORRELATION MATRIX

A. Self-consistency analysis

There are two methods for computing the first and second order moments of the state variables of Eq. (1): either directly from the differential equations for the moments, or by adding up the contribution of the different points in the distribution, each being separately evaluated using the moments equations. The self-consistency analysis consists of comparing the two methods.

A priori, the first method, which evaluates directly the moments appears more simple and efficient than the second which is using the same evaluation from the moments equations and the calculation of an integral. However, the self-consistency analysis provides a method to check how well the Gaussian assumption holds. Furthermore, the method is also the basis for the semianalytical computation of auto- and cross correlations of the state variables, as developed in Sec. III B. In the following, we first detail the second method.

We denote by $Q_t(u,v)$ the probability density function (pdf) of the joint distribution of (x_t,y_t). Under the Gaussian assumption, Q_t is Gaussian $N(\mu(t),\Sigma(t))$, where $\mu=(\mu_1(t),\mu_2(t))$ is the mean, and

$$\Sigma=\begin{pmatrix}\sigma_1 & \sigma_{12}\\ \sigma_{12} & \sigma_2\end{pmatrix} \tag{5}$$

is the covariance matrix.

The key observation for the second method for the evaluation of the moments is that

$$\begin{aligned}\mu_1(t+\tau)&=E[x(t+\tau)]\\ &=\int_{-\infty}^{+\infty}\int_{-\infty}^{+\infty}E[x(t+\tau)|x(t)=u,y(t)=v]\\ &\quad\times Q_t(u,v)dudv\\ &=\int_{-\infty}^{+\infty}\int_{-\infty}^{+\infty}m_1[\tau|x=u,y=v]Q_t(u,v)dudv,\end{aligned} \tag{6}$$

where $m_1(\tau|x=u,y=v)$ represents the value at time τ of the solution of the moments equations with initial conditions: $m_1(0)=u$, $m_2(0)=v$, $S_1(0)=S_2(0)=C_{12}(0)=0$. In other words, with the second method one derives the moments as a weighted average of individual solutions of the moments equations. The self-consistency analysis consists in comparing $\mu_1(t+\tau)$ from Eq. (6) with $m_1(t+\tau)$ the value of the solution of the moments equations satisfying $m_1(t)=\mu_1(t)$, $m_2(t)=\mu_2(t)$, $S_1(t)=\sigma_1(t)$, $S_2(t)=\sigma_2(t)$, $C_{12}(t)=\sigma_{12}(t)$ (i.e., going through Q_t at time t).

A similar analysis can be applied to all variables so that we obtain the following self-consistency conditions:

$$m_1(t+\tau)=\mu_1(t+\tau)=\int_{-\infty}^{+\infty}\int_{-\infty}^{+\infty} m_1[\tau|x=u,y=v]Q_t(u,v)dudv,$$

$$m_2(t+\tau)=\mu_2(t+\tau)=\int_{-\infty}^{+\infty}\int_{-\infty}^{+\infty} m_2[\tau|x=u,y=v]Q_t(u,v)dudv,$$

$$S_1(t+\tau)=\sigma_1(t+\tau)=\int_{-\infty}^{+\infty}\int_{-\infty}^{+\infty}(S_1[\tau|x=u,y=v]+m_1^2[\tau|x=u,y=v])Q_t(u,v)dudv-\mu_1^2(t+\tau),$$

$$S_2(t+\tau)=\sigma_2(t+\tau)=\int_{-\infty}^{+\infty}\int_{-\infty}^{+\infty}(S_2[\tau|x=u,y=v]+m_2^2[\tau|x=u,y=v])Q_t(u,v)dudv-\mu_2^2(t+\tau),$$

$$C_{12}(t+\tau)=\sigma_{12}(t+\tau)=\int_{-\infty}^{+\infty}\int_{-\infty}^{+\infty}(C_{12}[\tau|x=u,y=v]+m_1[\tau|x=u,y=v]m_2[\tau|x=u,y=v])$$
$$\times Q_t(u,v)dudv-\mu_1(t+\tau)\mu_2(t+\tau). \quad (7)$$

Using the marginal and the conditional distributions of x_t and y_t instead of the joint distribution Q_t, it is possible to derive another set of self-consistency conditions. We denote by $q_t^x(u)=\int Q_t(u,v)dv$ and $q_t^y(v)=\int Q_t(u,v)du$ the pdfs of x_t and y_t. These are Gaussians $N(\mu_1,\sigma_1)$ and $N(\mu_2,\sigma_2)$ (in our notation, the σ_i are variances). The conditional distributions, with pdfs $q_t^x(v|u)$ and $q_t^y(v|u)$ (i.e., the probability that $y=v$, given that $x=u$ and vice versa), are also Gaussians $N(\mu_2+(u-\mu_1)\sigma_{12}/\sigma_1,\sigma_2-\sigma_{12}/\sigma_1)$ and $N(\mu_1+(v-\mu_2)\sigma_{12}/\sigma_2,\ \sigma_1-\sigma_{12}/\sigma_2)$. Using these, we can rewrite Eq. (6) as

$$\begin{aligned}\nu_1(t+\tau)&=E[x(t+\tau)]\\&=\int_{-\infty}^{+\infty}E[x(t+\tau)|x(t)=u]q_t^x(u)du\\&=\int_{-\infty}^{+\infty}m_1[\tau|x=u]q_t^x(u)du,\end{aligned} \quad (8)$$

where the change in notations is to distinguish the value obtained from Eq. (8) from the one obtained from Eq. (6), and $m_1[\tau|x=u]$ is the value at time τ of the solution of the moments equations with initial conditions $m_1(0)=u$, $m_2(0)=\mu_2(t)+(u-\mu_1(t))\sigma_{12}(t)/\sigma_1(t)$, $S_1(0)=0$, $S_2(0)=\sigma_2(t)-\sigma_{12}(t)/\sigma_1(t)$, and $C_{12}(0)=0$ [i.e., going initially through $q_t^x(v|u)$]. In this way, the first two self-consistency conditions, derived from the marginal and conditional distributions, can be given by

$$m_1(t+\tau)=\nu_1(t+\tau)=\int_{-\infty}^{+\infty}m_1[\tau|x=u]q_t^x(u)du,$$

$$m_2(t+\tau)=\nu_2(t+\tau)=\int_{-\infty}^{+\infty}m_2[\tau|y=v]q_t^y(v)du. \quad (9)$$

Similar equations can be derived for the other conditions.

In fact, there are other possibilities for the derivation of self-consistency equations, with Eq. (7) being the basic one. The two equations derived from the marginal and conditional distributions [Eq. (9)] were given because they open the way for the evaluation of the correlations using only the moments equations. This is described in the next section.

B. Auto- and cross correlations

In the following, we take advantage of Eq. (9) in order to evaluate the entries of the correlation matrix of the stochastic process (x_t,y_t) using only the moments equations. In other words, we use the estimates of the first and second order moments at a given time together with their dynamics in order to estimate the auto- and cross correlations of the variables x and y. These quantities are of prime importance in the characterization of stochastic processes, as, for instance, they entirely determine the properties of Gaussian processes and consequently the responses of linear systems, or weakly perturbed systems operating near the linear regimes, to noise.

Denoting by $R_{xx}(\tau)$ and $R_{xy}(\tau)$ the autocorrelation of x and its cross correlation with y, at lag τ, we have

$$\begin{aligned}R_{xx}(\tau)&=E[x(t)x(t+\tau)]-E[x(t)]E[x(t+\tau)]\\&=\int_{-\infty}^{\infty}E[x(t+\tau)|x(t)=u]uq_t^x(u)du-m_1^{*2}\\&=\int_{-\infty}^{\infty}m_1[\tau|x=u]uq_t^x(u)du-m_1^{*2},\end{aligned}$$

$$\begin{aligned}R_{xy}(\tau)&=E[x(t)y(t+\tau)]-E[x(t)]E[y(t+\tau)]\\&=\int_{-\infty}^{\infty}m_2[\tau|x=u]uq_t^x(u)du.\end{aligned} \quad (10)$$

Similar expressions can be written for R_{yy} and R_{yx}, the autocorrelation of y and its cross correlation with x.

Figure 2 shows the results of numerical resolutions of Eq. (10) (thick solid lines) together with the same quantities estimated from simulations of the stochastic FHN (thin dashed lines). Overall, despite a quantitative underestimation at short time lags, the moments equations reproduce the main

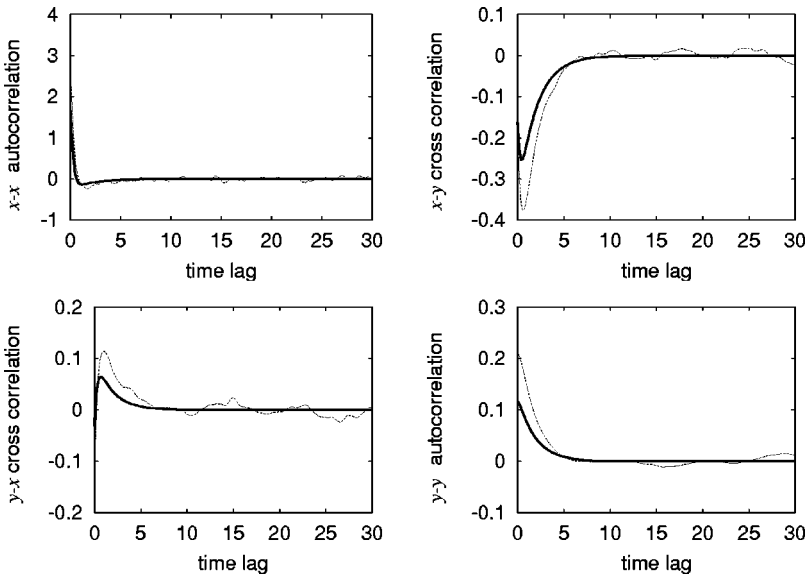

FIG. 2. Auto- and cross correlations of the FHN model as a function of time lag. Abscissas in all panels are time in milliseconds. Ordinates are in abritrary units and represent R_{xx} (top left panel), R_{xy} (top right panel), R_{yx} (bottom left panel), and R_{yy} (bottom right panel), respectively. Thick solid and thin dotted curves in each panel are the correlations computed from conditional moments and simulations, respectively. Model parameters used in this and the subsequent figures are $a=-1$, $b=0$, $c=3$, $e=-0.333\,333$, $f=-0.266\,666$, $q=0.233\,333$, and $h=3$. Noise level is $\sigma=0.05$ and constant current is $I=0$. For the conditional moments, 166 initial points were taken within $[m_1^*-5S_1^*, m_1^*+5S_1^*]$ and $[m_2^*-5S_2^*, m_2^*+5S_2^*]$. The simulation started at resting state. After free running for 500 ms, correlations were averaged over a duration of 10 000 ms. The simulation was run using the standard Euler method with the same time step as in Fig. 1.

qualitative aspects of the correlations, such as the rapid stabilization of these quantities to zero, following a pronounced initial increase and decrease in R_{yx} and R_{xy} (a less marked initial decrease is also present in R_{xx}). These results support our point that the revised moments equations are suitable for the analysis of the qualitative aspects of stationary distributions of the variables. This is done in the following.

IV. STOCHASTIC BIFURCATION

A bifurcation in a deterministic system is a qualitative change in the asymptotic dynamics, and it usually occurs when a parameter is moved across a critical value. Figure 4 represents the well-known bifurcation diagram of the deterministic FHN for the control parameter I (constant stimulation intensity). The system stabilizes at an equilibrium point at low and large current intensities, and displays periodic oscillations in the intermediate range of currents. These oscillations arise through Hopf bifurcations (for a recent comprehensive study of the bifurcations of the FHN please refer to [15]).

Qualitative changes in the behavior of stochastic systems due to a parameter modification can also be classified in terms of bifurcations. In this respect, phenomenological stochastic bifurcations refer to qualitative changes in the stationary distribution of the variables. Typical examples are when the number of modes of the distributions change, or that a single peak distribution becomes crater-like [10]. In contrast with deterministic bifurcations, phenomenological stochastic bifurcations may occur in a bifurcation interval rather than at a critical parameter value. In other words, the transition between two qualitatively different stationary distributions proceeds progressively when the bifurcation parameter is varied within the bifurcation interval.

We show that the noisy FHN undergoes a transition resembling such a bifurcation as either the noise intensity or the current amplitude is varied. Histograms illustrating the stationary distribution of x at three noise levels are shown in the top three panels of Fig. 3. At low noise, units are distributed in a Gaussian form around the resting state (left panel). As we increase the noise, a small proportion of units appear at the lower end of the Gaussian and at high values near the maximum of a discharge (middle panel). At high noise, this proportion becomes significant (right panel), thus the distribution is no longer Gaussian-like, and in fact presents a second mode.

The continuous effect of noise on the shape of the distribution is shown in the second row panel. The thick solid line represents the top and bottom limits and the thin dashed line represents the average value at each corresponding noise intensity. In this sense, this representation is reminiscent of the deterministic bifurcation diagram (Fig. 4) which also showed upper and lower values of x during oscillations. Up to an intermediate noise level (about $\sigma=0.2$), the distribution widens linearly as the noise is increased, while the center remains near the resting state. This property is reminiscent of a linear system. As noise is further increased, within a relatively narrow range of noise (about $0.2<\sigma<0.3$), the distribution widens markedly as depicted by the thick lines suddenly curving towards lower and higher values. Despite the asymmetric change in the boundaries, the average stays near the resting state, which is in agreement with the observation reported in the previous paragraph that, from this region, the distribution is non-Gaussian. At the high noise regime, the boundaries become almost parallel to the horizontal axis. This is due to the fact that changes in the noise intensity at this regime do not affect the qualitative shape of the distribution.

The changes in the distributions of the variable x depicted above are also present in the joint distribution of the two variables x and y which are presented at various noise levels and constant current (nine bottom panels in Fig. 3). Without constant current input, the distribution at low noise is close to a Gaussian centered at the stable equilibrium (left column, top panel). As the noise is increased, a small proportion appears along the discharge orbit (top row, middle panel). At a high noise level, the proportion along the orbit is significantly visible, and the distribution no longer resembles that

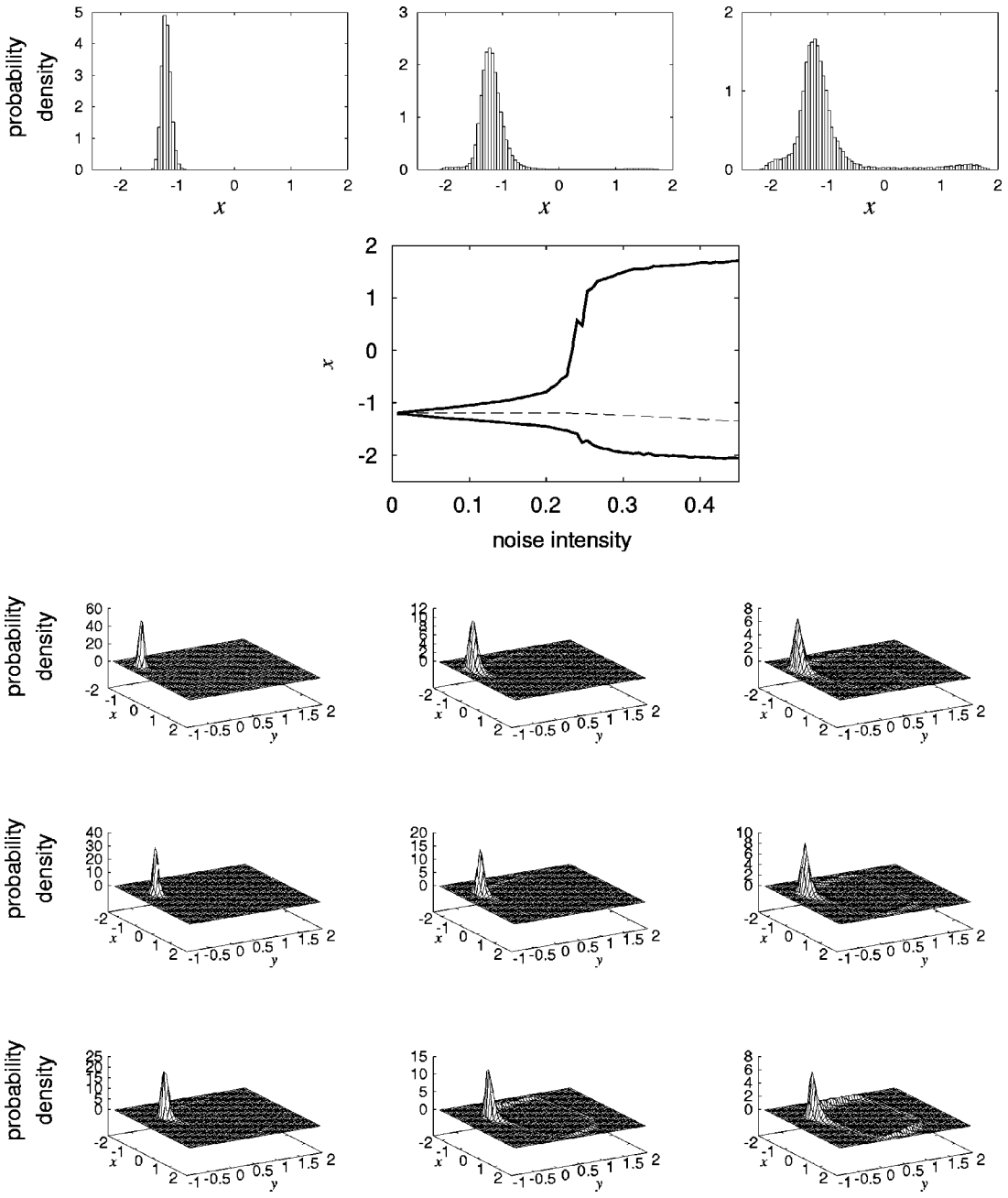

FIG. 3. The effect of noise on the stationary distribution of FHN models. The top three panels are the histograms of the value x (the sign of x is inverted so that discharging units appear at high positive values). The noise intensity (standard deviation of white Gaussian noise) is increased as $\sigma=0.133\,333$ (left panel), 0.266 666 (middle panel), and 0.333 333 (right panel). 100 000 units were sampled from simulations which all started at $x=y=1$ and run for 100 ms. The bin size of the histograms is 0.05. The abscissas of these panels are in arbitrary units (a.u.), the ordinates are counts divided by bin width (in a.u.). In the second row panel, top and bottom boundaries (thick solid lines) and the average (thin dashed line) of x is plotted as function of noise intensity. 10 000 units were simulated. Boundaries are determined such that one percent are beyond the top and another one percent are beyond the bottom boundaries. The abscissas and the ordinate are in arbitrary units. The bottom nine three-dimensional plots are the histograms of the joint distribution plotted on the x-y phase plane. Constant current intensity is increased from top to bottom as $I=0$ (top row), 0.5 (second row), and 1 (bottom row). Noise intensity is increased from left to right, i.e., $\sigma=0.133\,333$ (top row, left panel), 0.333 333 (top row, middle panel), 0.4 (top row, right panel), 0.133 333 (second row, top panel), 0.2 (second row, middle panel), 0.266 666 (second row, right panel), 0.033 333 (bottom row, left panel), 0.066 666 (bottom row, middle panel), and 0.166 666 (bottom row, right panel). The number of simulated units are $N=100\,000$ (top row) and $N=20\,000$ (second and bottom rows). Bin size of the x axis is 0.1 and the y axis is 0.06. The two horizontal axes of these panels are in arbitrary units, while the vertical axis are in counts per bin surface (a.u.). Model parameters and simulation time step is the same as in Fig. 2.

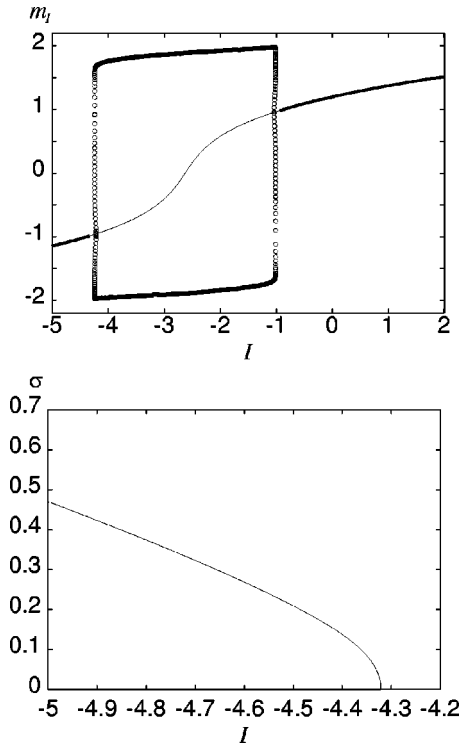

FIG. 4. Connection of deterministic and stochastic bifurcation in FHN model. Bifurcation of the approximation in Eq. (4) as constant current input is changed when the noise intensity is zero (upper panel). Abscissa is current and ordinate is m_1. Both are in arbitrary units. The thick solid lines represent the stable solutions and the thin line represents the unstable solution. The closed circles represent the extrema of stable periodic solutions and open circles represent those of unstable periodic solutions. The curve in the bottom panel indicates the phase boundary in the I-σ two parameter plane. The intersection of the curve with the abscissa corresponds to the first Hopf bifurcation point in the upper panel. The abscissa is current and the ordinate is noise intensity, and both are in arbitrary units.

of a Gaussian (top row, right panel). When an intermediate constant current I is injected, the distribution along the orbit appears at lower noise intensity (second row, left and middle panels). This is due to the fact that the stable equilibrium is shifted closer to threshold, so that discharge is induced by smaller perturbations. When the injected constant current is close to threshold, the distribution along the orbit is visible at even very small noise (bottom row, left panel). At this current intensity the distribution along the orbit is clearly visible at larger noise intensities (bottom row, middle and right panels).

In summary, our numerical investigations establish that the noisy FHN model undergoes a transition resembling a phenomenological stochastic bifurcation as either the noise intensity or the constant current level are increased. This bifurcation is characterized by a radical change of shape of the stationary distribution of the variables occurring over a short range of parameters. Prior to this bifurcation, the distributions take on a Gaussian form. Following it, the individual distributions of the variables become bimodal, and their joint distribution presents a circle like locus of local maxima along the discharge trajectory.

The moments equations approximate well the moments of the variables distributions prior to the bifurcation, in the Gaussian regime. For noise intensities or constant currents beyond the bifurcation range, the moments equations can only provide a satisfactory estimate during a transient time, and not for the long term values of the moments, because the corresponding stationary distributions are no longer Gaussian-like. This phenomenon in fact results in a change of the asymptotic behavior of the moments equations, which can be analyzed in terms of deterministic bifurcations.

This point is illustrated in Fig. 4 (bottom panel) which shows the two-parameter bifurcation diagram of the moments equations for the control parameters noise and current intensities. The line crossing the diagram and connecting the y axis to the x axis represents the location at which the moments equations undergo a Hopf bifurcation. For noise and current intensities enclosed within this line and the two axes, the moments equations stabilize at a stable equilibrium point, reflecting the fact that the stationary distributions are Gaussian. Beyond this bifurcation point, they display periodic oscillations over a narrow range. Further away, they undergo other bifurcations (not shown) whose nature is not of importance, because the first Hopf bifurcation indicates that beyond this limit, the Gaussian approximation breaks down in the stationary regime. Therefore the phenomenological stochastic bifurcation characterizing the transition from Gaussian to non-Gaussian stationary distributions appears as a Hopf bifurcation of the moments equations.

The Hopf bifurcation line confirms the observations based upon numerical simulations that the noise range at which the stochastic bifurcation occurs decreases with increasing current intensity. In fact, the intersection point between the Hopf line and the y axis in Fig. 4 corresponds exactly to the Hopf bifurcation point of the deterministic FHN, suggesting that the stochastic bifurcations are in fact an extension of this deterministic bifurcation in the noisy system.

V. DISCUSSION

In a previous work, we reported the change of behavior in stochastic HH equations [9] that strongly resembled a phenomenological stochastic bifurcation, and which accounted for the noise enhanced discharge time precision in neuronal ensembles. The purpose of the present work was twofold: (i) develop a systematic method for the analysis of such noise induced changes, and (ii) apply it to a prototype of an excitable system, namely the FHN, to show that the phenomenon observed in the HH model can be expected to occur in other excitable systems.

The main step in this process was to obtain a deterministic system whose bifurcations would reflect the phenomenological stochastic bifurcation of the noisy system. While this constitutes a standard approach for the analysis and classification of the behavior of noisy systems, our method differs from previous studies. Indeed, mainly this problem has been tackled in systems composed of interacting units. For these, it is possible to obtain a deterministic description of the macroscopic behavior of the system in the limit where the system

has infinitely many interacting components [16]. However, this method is not appropriate for the analysis of the phenomenological stochastic bifurcations at the single unit level, such as the ones studied in the present work. For this reason, we proceeded along a different approach which consisted of using the moments equations for the determination of stochastic bifurcations.

In this respect, the first part of our work was methodological and consisted of the modification of the moments equations obtained using the RT method to render them suitable for our purpose. In the process, we also derived; (i) a general method for the evaluation of such equations for general HH type models (Appendix B), (ii) self-consistency conditions for the moments equations, and (iii) general expression of the auto- and cross correlations using the moments equations. These results are general and hold beyond the example of the FHN model considered.

The second part of our work presented numerical evidence for stochastic bifurcation in the FHN, which confirmed the generality of the observations made in the HH model [9]. It further argued that this change of behavior was reflected in a deterministic Hopf bifurcation in the corresponding moments equations. While our previous work was concerned only with the influence of noise, the present one reported the analysis of the joint effect of noise level together with constant current intensity. This in turn revealed that a similar phenomenological stochastic bifurcation takes place when at fixed noise level the intensity of the constant current stimulation is increased. This hint to the similarity between the stochastic bifurcation and the Hopf bifurcation separating excitable and oscillating regimes in the FHN was confirmed in the bifurcation diagram of the moments equations.

In conclusion, the present study improved on the RT approximation for the derivation of the moments equations of stochastic systems and developed an application for it, namely in the analysis of stochastic bifurcations. The example presented here was that of the FHN model and was motivated by the fact that stochastic bifurcations in excitable systems such as neurons can play a functional role in signal processing. Nevertheless, the methodology developed is general and can be applied to the analysis of noise related changes in other classes of systems.

ACKNOWLEDGMENT

S.T. would like to thank T. Shimokawa for helpful discussions.

APPENDIX A: APPROXIMATIONS IN A GENERAL SYSTEM

Rodriguez and Tuckwell's approximation. We first remind Rodriguez and Tuckwell's [11] approximation of the moments. Let us consider an n-dimensional random process $\mathbf{x}(t)=(x_1(t),\ x_2(t),\ \ldots,x_n(t))$ with a (close to) Gaussian pdf $p(\mathbf{u},t)=p(u_1,u_2,\ \ldots,u_n,t)$. Then, using a second order Taylor expansion of p around its mean $\mathbf{m}(t)$, the expectation of an arbitrary function $G(\mathbf{x},t)$ can be expressed as

$$E[G(\mathbf{x},t)]=\int\int\cdots\int_{-\infty}^{\infty}G(\mathbf{u},t)p(\mathbf{u},t)d\mathbf{u} \tag{A1}$$

$$\approx G(\mathbf{m},t)+\frac{1}{2!}\sum_{l=1}^{n}\sum_{k=1}^{n}\frac{\partial^2 G}{\partial u_l\partial u_k}(\mathbf{m},t)\cdot C_{lk}, \tag{A2}$$

where $C_{lk}=E[(x_l-m_l)(x_k-m_k)]$ are the second order moments. This approximate expression for the expectation lies at the heart of the RT method [11] because it allows a systematic derivation of the equations for the dynamics of the first and second order moments as a function of only these same variables.

G method. When the function G in Eq. (A1) is a polynomial, its expectation can be expressed exactly in terms of the first and second order moments using the fact that all higher moments of a Gaussian distribution can be written in terms of these, as

$$E[x_1x_2\cdots x_j]=\sum_{\text{all pairing}}\prod_{(l,k)}C_{lk}\quad \text{if } j \text{ is even}$$

$$=0\quad \text{if } j \text{ is odd}, \tag{A3}$$

where we take $j/2\,(j>2)$ pairs of (l,k) for the product and all $(j-1)(j-3)\cdots 3\cdot 1$ combinations of pairs for the summation. In this way, one avoids using Taylor expansions, and gains higher approximation accuracy.

APPENDIX B: MOMENTS OF THE GENERAL HODGKIN-HUXLEY-TYPE MODEL

In [13], Rodriguez and Tuckwell derive the moments equations for the standard HH equations [17] using the second order Taylor expansion mentioned previously. In this appendix, we consider the case of general HH type equations of the form:

$$\frac{dV}{dt}=\sum_i g_i m_i^p h_i^q(V_i-V)+I+\xi(t), \tag{B1}$$

$$\frac{dx}{dt}=\alpha_x(V)-\gamma_x(V)x, \tag{B2}$$

where the variables V, m_i, and h_i are the membrane potential, and the activation and inactivation of the ith ion current. V_i is the reversal potentials and $g_i=G_i/C_m$ is the corresponding maximal conductances G_i normalized by the membrane capacitance C_m. p and q are integers that depend on i ($q=0$ if there is no inactivation). $\xi(t)$ represents white Gaussian noise satisfying $E(\xi(t))=0$ and $E(\xi(t)\xi(s))=\sigma^2\delta(t-s)$. x in Eq. (B2) represents gating variables denoted as m_i and h_i in Eq. (B1). $\alpha_x(V)$ and $\gamma_x(V)$ are auxiliary functions of V that determine the dynamics of gating variables.

We denote the first and second order moments associated with the state variables of Eqs. (B1) and (B2) as $\overline{V}$, $\overline{x}$, S_V, S_x, C_{Vx}, and C_{xy}. The moments equations are given by

$$\frac{d\overline{V}}{dt}=\sum_i g_i E[\overline{m_i^p}\,\overline{h_i^q}(V_i-\overline{V})]+I, \tag{B3}$$

$$\frac{dS_V}{dt}=2\sum_i g_i E[(V-\overline{V})\overline{m_i^p}\,\overline{h_i^q}(V_i-V)]+\sigma^2, \tag{B4}$$

$$\frac{dC_{Vx}}{dt}=E\left[(x-\overline{x})\sum_i g_i m_i^p h_i^q (V_i-V)\right] + E[(V-\overline{V})(\alpha_x(V)-\gamma_x(V)\cdot x)], \tag{B5}$$

$$\frac{d\overline{x}}{dr}=E[\alpha_x(V)-\gamma_x(V)x], \tag{B6}$$

$$\frac{dS_x}{dt}=2[(x-\overline{x})(\alpha_x(V)-\gamma_x(V)\cdot x)], \tag{B7}$$

$$\frac{dC_{xy}}{dt}=E[(x-\overline{x})(\alpha_y(V)-\gamma_y(V)\cdot y)] + E[(y-\overline{y})(\alpha_x(V)-\gamma_x(V)\cdot x)]. \tag{B8}$$

The right-hand sides of the first two equations as well as the first term in the right-hand side of the third one are expectations of polynomials and are therefore entirely determined using the G method and Eq. (A3). The remaining terms can be treated using the Taylor expansion, up to an arbitrary order, and can be expressed as one of the three general expansions provided below:

$$E[g(x_1)]=\sum_{k\geqslant 0}\frac{1}{2^k k!}g^{(2k)}(\overline{x_1})R_{11}^k, \tag{B9}$$

$$E[g(x_1)x_2]=R_{12}\sum_{k\geqslant 0}\frac{1}{2^k k!}g^{(2k+1)}(\overline{x_1})R_{11}^k, \tag{B10}$$

$$E[g(x_1)x_2x_3]=\sum_{k\geqslant 0}\frac{1}{2^k 2!}(R_{11}R_{23}+2kR_{12}R_{13}) \times g^{(2k)}(\overline{x_1})R_{11}^{k-1}, \tag{B11}$$

where $\{x_i\}$ form a Gaussian vector with covariance matrix $[R_{ij}]$, g is some arbitrary function, and $g^{(k)}$ is its kth derivative.

In this way, combining the G method and the Taylor expansion, one can derive the moments equations, Eqs. (B3)–(B8), for any HH type equation up to an arbitrary order.

[1] J. P. Segundo, J.-F. Vibert, K. Pakdaman, M. Stiber, and O. Diez-Martínez, in *Origins: Brain and Self Organization*, edited by K. Pribram (Lawrence Erlbaum, Hillsdale, NJ, 1994); J. K. Douglass, L. Wilkens, E. Pantazelou, F. Moss, Nature (London) (London) **365**, 337 (1993); J. E. Levin and J. P. Miller, *ibid.* **380**, 165 (1996); D. F. Russell, L. A. Wilkens, and F. Moss, *ibid.* **402**, 291 (1999); C. Ivey, A. V. Apkarian, and D. R. Chialvo, J. Neurophysiol. **79**, 1879 (1998); J. J. Collins, T. T. Imhoff, and P. Grigg, *ibid.* **76**, 642 (1996).

[2] H. C. Tuckwell, *Stochastic Processes in the Neurosciences* (SIAM, Philadelphia, 1989).

[3] A. V. Holden, Models of the stochastic activity of neurones, Lecture Notes in Biomathematics, Vol. 12 (Springer, Berlin, 1976).

[4] L. M. Ricciardi, A. D. Crescenzo, V. Giorno, and A. G. Nobile, Math. Japonica **50**, 247 (1999); P. Lansky and S. Sato, J. Periph. Nervous System **4**, 27 (1999).

[5] A. R. Bulsara, T. C. Elston, C. R. Doering, S. B. Lowen, and K. Lindenberg, Phys. Rev. E **53**, 3958 (1996); T. Shimokawa, A. Rogel, K. Pakdaman, and S. Sato, Phys. Rev. E **59**, 3461 (1999); T. Shimokawa, K. Pakdaman, and S. Sato, *ibid.* **60**, R33 (1999); **59**, 3427 (1999); T. Shimokawa, K. Pakdaman, T. Takahata, S. Tanabe, and S. Sato, Biol. Cybern. **83**, 327 (2000).

[6] H. Lecar and R. Nossal, Biophys. J. **11**, 1048 (1971); H. Lecar, Biophys. Soc. Abstracts **13**, 158a (1973).

[7] X. Pei, L. Wilkens, and F. Moss, Phys. Rev. Lett. **77**, 4679 (1996).

[8] A. Longtin, Chaos, Solitons Fractals **11**, 1835 (2000); J. J. Collins, C. C. Carson, and T. T. Imhoff, Nature (London) **376**, 236 (1995); K. Wiesenfeld, D. Pierson, E. Pantazelou, C. Dames, and F. Moss, Phys. Rev. Lett. **72**, 2125 (1994).

[9] S. Tanabe, S. Sato, and K. Pakdaman, Phys. Rev. E **60**, 7235 (1999).

[10] L. Arnold, *Random Dynamical Systems* (Springer-Verlag, Berlin, 1998).

[11] R. Rodriguez and H. C. Tuckwell, Phys. Rev. E **54**, 5585 (1996).

[12] H. C. Tuckwell and R. Rodriguez, J. Comput. Neurosci. **5**, 91 (1998).

[13] R. Rodriguez and H. C. Tuckwell, BioSystems **48**, 187 (1998).

[14] R. A. FitzHugh, Biophys. J. **1**, 445 (1961); J. Nagumo, S. Arimoto, and S. Yoshizawa, Proc. IRE **50**, 2061 (1962).

[15] B. Barnes and R. Grimshaw, J. Aust. Math. Soc. B, Appl. Math. **38**, 427 (1997).

[16] S. Tanabe, T. Shimokawa, S. Sato, and K. Pakdaman, Phys. Rev. E **60**, 2182 (1999); J. Pham, K. Pakdaman, and J.-F. Vibert, *ibid.* **58**, 3610 (1998); C. Kurrer and K. Schulten, *ibid.* **51**, 6213 (1995); S. Shinomoto and Y. Kuramoto, Prog. Theor. Phys. **75**, 1105 (1986); H. Sakaguchi, S. Shinomoto, and Y. Kuramoto, *ibid.* **79**, 600 (1988); M. Shiino, Phys. Rev. A **36**, 2393 (1987); P. Jung, U. Behn, E. Pantazelou, and F. Moss *ibid.* **46**, R1709 (1988).

[17] A. L. Hodgkin and A. F. Huxley, J. Physiol. (London) (London) **117**, 500 (1952).